

Observation of Long Spin-Relaxation Times in Bilayer Graphene at Room Temperature

T.-Y. Yang,^{1,2,*} J. Balakrishnan,^{3,†} F. Volmer,^{1,2} A. Avsar,³ M. Jaiswal,³ J. Samm,^{1,2} S.R. Ali,^{1,2} A. Pachoud,³ M. Zeng,³ M. Popinciuc,^{1,2} G. Güntherodt,^{1,2} B. Beschoten,^{1,2,‡} and B. Özyilmaz^{3,4,§}

¹*Institute of Physics, RWTH Aachen University, 52074 Aachen, Germany*

²*JARA: Fundamentals of Future Information Technology, 52074 Aachen, Germany*

³*Department of Physics, National University of Singapore, Singapore 117542, Singapore*

⁴*NanoCore, National University of Singapore, Singapore 117576, Singapore*

(Received 27 November 2010; published 21 July 2011)

We report on the first systematic study of spin transport in bilayer graphene (BLG) as a function of mobility, minimum conductivity, charge density, and temperature. The spin-relaxation time τ_s scales inversely with the mobility μ of BLG samples both at room temperature (RT) and at low temperature (LT). This indicates the importance of D'yakonov-Perel' spin scattering in BLG. Spin-relaxation times of up to 2 ns at RT are observed in samples with the lowest mobility. These times are an order of magnitude longer than any values previously reported for single-layer graphene (SLG). We discuss the role of intrinsic and extrinsic factors that could lead to the dominance of D'yakonov-Perel' spin scattering in BLG. In comparison to SLG, significant changes in the carrier density dependence of τ_s are observed as a function of temperature.

DOI: 10.1103/PhysRevLett.107.047206

PACS numbers: 85.75.-d, 72.25.Dc, 72.25.Rb, 72.80.Vp

The demonstration of micrometer long spin-relaxation lengths in graphene by Tombros *et al.* [1] has made this 2D material a promising candidate for spintronics applications. So far most spin transport studies have focused on single-layer graphene (SLG) [1–12] while the equally important bilayer graphene (BLG) has not yet received much attention. This is surprising since BLG has unique electronic properties which differ greatly from those of SLG (effective mass of carriers, electric-field induced band gap) and also differ from those of regular 2D electron gases (chirality) [13,14]. It is currently believed that spin relaxation in SLG is limited by the momentum scattering from extrinsic impurities [2,4,15]. Unlike SLG, the scattering from such charged impurities is reduced by the enhanced screening in BLG [16]. This leads to a relative importance of short-range (SR) scatterers in determining the transport properties such as the temperature (T) and charge carrier density (n) dependence of the BLG conductivity (σ) [16,17]. Interlayer hopping also plays an important role in the electronic properties of BLG and is predicted to cause an enhanced intrinsic spin-orbit (SO) coupling (up to 0.1 meV in clean samples) in comparison to SLG [18]. The unique electronic properties of BLG may offer new avenues to manipulate the spin degree of freedom.

In this Letter we report on spin transport studies in BLG both at room temperature (RT) and at low temperature (LT) using MgO barriers. Spin-valve devices in the nonlocal geometry are fabricated on two types of MgO-covered exfoliated graphene samples using standard e -beam lithography techniques. For global MgO samples, MgO covers the entire graphene surface while for local MgO samples the MgO is only under the Co electrodes. This is followed by the evaporation of the ferromagnetic contacts (Co) [19].

The atomic force microscope (AFM) image after MgO deposition and the scanning electron microscope (SEM) image after the device fabrication for one of the BLG samples are shown in Fig. 1. In order to investigate the nature of spin scattering in BLG, we have evaluated the spin-relaxation time τ_s as a function of four parameters: (1) the field-effect mobility μ , (2) the minimum conductivity σ_{\min} , (3) the charge carrier density n , and (4) the temperature T in the range of 5 to 300 K. Among these parameters the mobility dependence of τ_s provides the most direct way to deduce the dominant scattering mechanism: a linear dependence of τ_s on μ (or τ_p) is *a priori* suggestive of an Elliott-Yafet (EY) spin scattering mechanism [20], while the inverse relation ($\tau_s \propto 1/\mu \propto 1/\tau_p$) will indicate the dominance of D'yakonov-Perel' (DP)-like spin scattering mechanisms [21]. In general, both mechanisms could be simultaneously relevant. For this study, we have selected

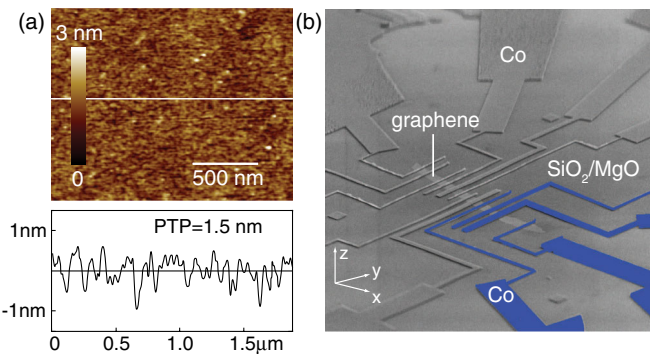


FIG. 1 (color online). (a) AFM image of a BLG sample after MgO deposition: rms roughness ~ 0.3 nm. (b) SEM image of a BLG sample with multiple nonlocal spin valves.

representative 17 devices on 6 BLG samples whose field-effect mobilities vary by more than 1 order of magnitude, from $\mu \sim 200 \text{ cm}^2/\text{Vs}$ to $8000 \text{ cm}^2/\text{Vs}$. The effect of impurity scattering on τ_s can also be deduced from σ_{\min} , which depends on impurity concentration. The third parameter chosen is the charge carrier density: the density dependence of τ_s and τ_p is used to identify the spin scattering mechanism in SLG (EY). In BLG, the τ_p is often taken to be a constant under the assumption of charge scattering from weak short-range scatterers and charged impurities. Recent LT experiments [22] indicate, however, that the density dependent τ_p results from strong short-range scattering in BLG. As a general trend in most of our samples σ is linear at high carrier density $1\text{--}3 \times 10^{12} \text{ cm}^{-2}$ [see Fig. 2(a) upper panel]. As the variation of τ_p is weak in this charge density range, we particularly compare the product $\tau_s \tau_p$ and the ratio τ_s/τ_p as a function of carrier density n ; the former is expected to be a constant for DP whereas the latter is a constant for EY. The fourth parameter chosen is temperature: unlike SLG, there is a strong temperature dependence of charge transport in BLG, which should also reflect itself in spin transport parameters.

We first characterize the BLG conductivity as a function of back gate voltage [Fig. 2(a)]. As also observed by other groups [7,9], the graphene samples are electron doped in the spin-valve configuration due to doping by the Co/MgO barrier [23]. The nonlocal spin signal (ΔR) is measured by in-plane magnetic field loops. A clear bipolar spin transport signal is observed at RT [see Fig. 2(b)], with a positive value of the nonlocal resistance for parallel alignment of

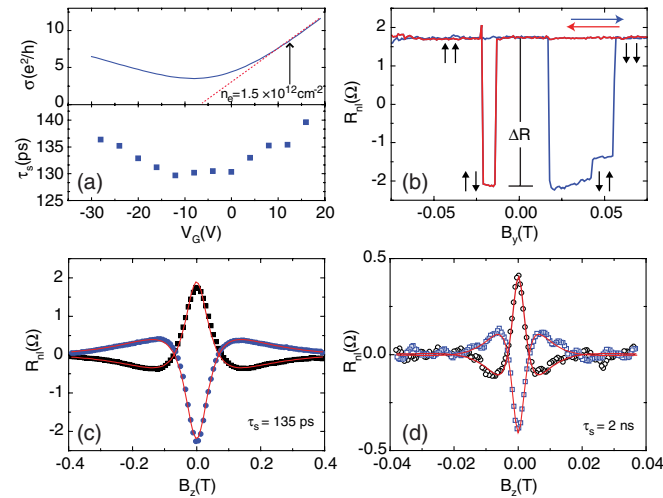


FIG. 2 (color online). RT data: (a) σ vs V_G and τ_s vs V_G for BLG. (b) Nonlocal resistance as a function of the in-plane magnetic field $B_y(T)$. The horizontal arrows show the field sweep direction while the vertical arrows show the relative magnetization orientations of the injector and detector electrodes. Hanle precession measurement for a perpendicular magnetic field $B_z(T)$ sweep for (c) the same sample with $\mu \sim 2000 \text{ cm}^2/\text{Vs}$ and (d) for a sample with $\mu \sim 300 \text{ cm}^2/\text{Vs}$.

the electrodes' magnetization and a negative resistance for the antiparallel alignment ($\Delta R = 4 \Omega$). To confirm the observed spin signals, conventional Hanle spin precession measurements [24] are performed at the same electron density of $n = 1.5 \times 10^{12} \text{ cm}^{-2}$ above which the conductance is linear and the mobility is well defined within the Boltzmann approximation [Figs. 2(c) and 2(b)]. The magnetic field dependence of the nonlocal resistance is fitted by

$$R_{nl} \propto \int_0^\infty \frac{1}{\sqrt{4\pi D_s t}} e^{-(L^2/4D_s t)} \cos(\omega_L t) e^{-t/\tau_s} dt, \quad (1)$$

where D_s is the spin-diffusion coefficient and $\omega_L = g\mu_B B/\hbar$ is the Larmor frequency for spin in an external magnetic field and thus gives the values for the spin parameters [24]. At $n = 1.5 \times 10^{12} \text{ cm}^{-2}$ we obtain a diffusion constant of $D_s = 0.0032 \text{ m}^2/\text{s}$ and a spin-relaxation time of $\tau_s = 135 \text{ ps}$ for a sample with $\mu = \Delta\sigma/e\Delta n = 2000 \text{ cm}^2/\text{Vs}$ [Fig. 2(c)]. The values give a spin-relaxation length of $0.7 \mu\text{m}$. The spin-relaxation time τ_s as a function of gate voltage (doping) is plotted in Fig. 2(a) (lower panel) showing an increase ($< 10\%$) of τ_s with doping, away from the charge neutrality point (CNP). This is qualitatively similar to the gate tunability of τ_s in SLG, although τ_s shows a weaker dependence in BLG at RT.

We next evaluate the dependence of τ_s on μ in the Boltzmann regime. As shown in Fig. 3(a) by a log-log plot, we observe an inverse dependence of τ_s on the mobility. Note that all data are taken at an electron density $n = 1.5 \times 10^{12} \text{ cm}^{-2}$. In samples with the highest mobility τ_s is only 30 ps. On the other hand, we observe a spin-relaxation time τ_s of up to 2 ns at RT for samples with the lowest mobilities (see corresponding Hanle curve in Fig. 2(d), [25]). Such values for τ_s are 1 order of magnitude longer compared to values reported so far in any SLG experiment. Furthermore, this strong variation of τ_s with μ offers the most direct evidence of the correlation between spin and charge transport. Since higher mobility

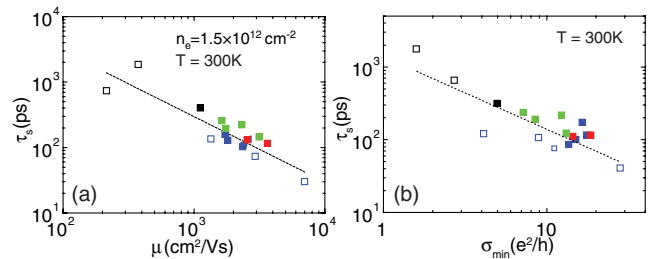


FIG. 3 (color online). Results of Hanle precession measurements at RT for 17 BLG spin devices with mobility varying from $200\text{--}8000 \text{ cm}^2/\text{Vs}$. The data points with the same symbol represent different junctions on the same sample. Open and closed symbols correspond to samples with global and local MgO, respectively. (a) τ_s taken at $n = 1.5 \times 10^{12} \text{ cm}^{-2}$ vs μ plotted on a log-log scale. (b) τ_s taken at the CNP vs σ_{\min} for BLG samples at RT.

samples will typically involve higher momentum relaxation time τ_p , assuming $\mu \propto \tau_p$ in the Boltzmann regime, the inverse dependence of τ_s on μ clearly demonstrates that the DP mechanism is the dominant spin scattering mechanism in BLG at RT.

The same plot of τ_s vs μ is also useful to elucidate the possible origin of the DP mechanism. For this, we first estimate the strength of spin-orbit (SO) coupling (Δ) in BLG using the expression $1/\tau_s = \Omega_{\text{eff}}^2 \tau_p = 4\Delta^2 \tau_p / \hbar^2$, where Ω_{eff} is the effective Larmor frequency of the precessing spins and Δ is the corresponding SO coupling strength [15]. The value Ω_{eff} is obtained from the τ_s vs μ data [Fig. 3(a)], $\Omega_{\text{eff}} = 407 \pm 25$ GHz, which gives $\Delta \sim 0.14 \pm 0.01$ meV. Additionally, Δ only weakly depends on temperature [19]. Therefore, it is unlikely that low energy phonons (such as acoustic phonons) are responsible for the observed spin scattering. The most important open question is whether this SO coupling is intrinsic or extrinsic in nature. The intrinsic SO coupling of BLG is expected to lead to $\Delta_{\text{intrinsic}}$ up to 0.1 meV in clean BLG samples [18]. While this is in good agreement with the value extracted from the τ_s vs μ plot, the influence of both the externally applied electric field and the role of adatoms cannot be excluded. Since interlayer hopping is involved in BLG, electric-field dependent modifications to the intrinsic SO coupling are expected. Adatoms, on the other hand, induce local curvature to an otherwise flat graphene lattice and can cause spin scattering by both EY and DP mechanism [11,15]. In SLG, the recent studies on the influence of external adatoms on spin transport also shows an increase in τ_s with increase in adatom concentration indicating a DP like scattering at LT [8]. However, in the case of BLG the role of the adatoms, in determining DP or EY spin scattering, might be even smaller due to a higher lattice stiffness [26], thus reducing the adatom induced SO coupling strength. Moreover, the effect of the charged impurities is also reduced due to enhanced screening in BLG. Thus the two prominent factors (charged impurities and adatoms) responsible for the spin scattering in SLG play a minor role in BLG which could also be the reason why we see longer spin-relaxation times in BLG.

We next evaluate the dependence of τ_s on the RT minimum conductivity σ_{min} and charge carrier density n of the BLG samples. The τ_s vs σ_{min} graph [Fig. 3(b)] indicates a decrease in τ_s with increasing σ_{min} . The value of σ_{min} at RT varies significantly between clean and dirty samples and is higher for cleaner samples [17,27]. The inverse dependence of τ_s on σ_{min} indicates a higher spin-relaxation time in dirtier samples. Therefore, this correlation is in good agreement with the above conclusion that DP spin scattering is dominant in BLG at RT. Finally, we analyze the weak dependence of τ_s on n for individual samples [Fig. 2(a)]. At first we note that at RT the density dependence of $\tau_p = \sigma m^* / ne^2$ shows a gradual decrease with increasing n in the density range $1-3 \times 10^{12} \text{ cm}^{-2}$ for

our samples [19]. In this range, the quantity $\tau_s \tau_p$ is almost constant ($\sim 4\%$ change with charge density) while τ_s / τ_p shows an increase of 28% with increasing charge density at RT. This is consistent with the dominance of the DP mechanism at RT.

Next we evaluate spin transport as a function of temperature. Here, it is important to note that for BLG [Fig. 4(b)], and unlike SLG [Fig. 4(c)], the charge transport already shows strong changes with decreasing temperature due to the thermally activated nature of carriers near the CNP [19,28]. We may expect these changes to be reflected in the spin transport, as the temperature is lowered. We first note that for charge transport, there are two distinct bilayer specific density regimes [Fig. 4(b) upper panel]: (A) $n > 1 \times 10^{12} \text{ cm}^{-2}$, involving temperature independent transport and (B) $n < 1 \times 10^{12} \text{ cm}^{-2}$, involving thermally activated transport [19]. For regime (A) away from the CNP the mobility is well defined. Here the τ_s can be easily evaluated, similar to the approach used for analyzing RT data. We measured eight devices in three samples with μ ranging from $700 \text{ cm}^2/\text{Vs}$ to $3800 \text{ cm}^2/\text{Vs}$ at $T = 5 \text{ K}$. The data plotted in Fig. 4(a), show that the inverse dependence of τ_s on μ persists down to 5 K, demonstrating DP as the dominant spin scattering mechanism even at LT. At the same time, we note that the density dependence of τ_s and τ_p is rather weak in the Boltzmann regime for $n > 1 \times 10^{12} \text{ cm}^{-2}$ and does not allow for a clear assignment of the dominant spin scattering mechanism. The quantities $\tau_s \tau_p$ and τ_s / τ_p show comparable small changes in this regime both at 50 K and at 5 K [19]. Therefore, in this density regime we are left only with the mobility dependence at LT.

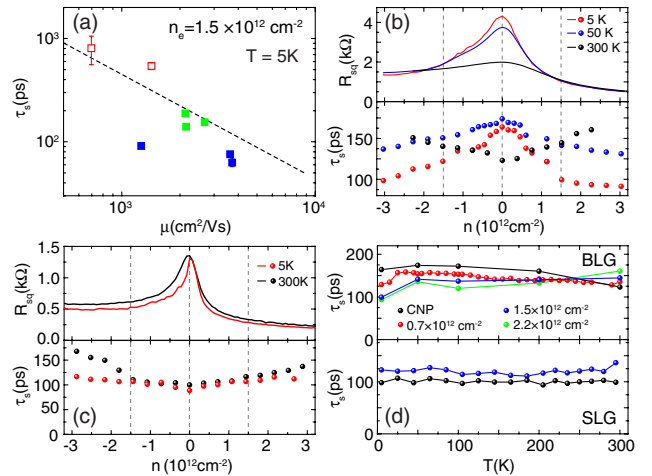


FIG. 4 (color online). (a) τ_s vs μ for 8 BLG junctions at 5 K. (b) Upper panel: R vs n for BLG; Lower panel: τ_s vs n for $T = 300 \text{ K}$, 50 K , and 5 K . (c) Upper panel: R vs n for SLG; lower panel: τ_s vs n for SLG at RT and at 5 K. (d) Upper panel: τ_s vs T for four densities, $n = \text{CNP}$, 0.7 , 1.5 , and $2.2 \times 10^{12} \text{ cm}^{-2}$. Lower panel: τ_s vs T for SLG at $n = \text{CNP}$, $1.5 \times 10^{12} \text{ cm}^{-2}$.

We finally consider the low density regime ($n < 1 \times 10^{12} \text{ cm}^{-2}$) around the CNP, involving the thermally activated behavior of the charge transport. Here, the minimum conductivity at CNP (σ_{\min}) is no longer a suitable parameter for scaling τ_s . The available σ_{\min} data scatters significantly at LT (not shown), but the overall variation in σ_{\min} is small compared to RT. This is not surprising since σ_{\min} is expected to take a disorder independent value of $3e^2/\pi h$ at $T = 0 \text{ K}$ [29]. Thus we are left only with the density dependence of τ_s to elucidate on what happens near the CNP at LT. This density dependence of τ_s at RT shows a minimum at CNP, as discussed above. As the temperature is lowered, this minimum in τ_s is gradually suppressed and the slope of $\tau_s(n)$ changes sign. Finally, at $T = 5 \text{ K}$ the density dependence of τ_s shows strong enhancement ($> 50\%$) near the CNP [Fig. 4(b), lower panel].

The key to understanding which spin scattering mechanism dominates at LT near CNP lies in the density dependence of τ_p . We note that $\tau_p = \sigma m^*/ne^2$ (Boltzmann approximation), estimated for our samples, gives a quantitative estimate only in the high density (Boltzmann) regime. Closer to the CNP, τ_p extracted from the above assumption shows an increase with decreasing density [19]. Recent detailed experiments on BLG at LT have shown that a divergence of τ_p near the CNP is indeed observed [19,22]. With this, a correlation of $\tau_s(n)$ with $\tau_p(n)$ suggests a transition from DP to EY spin scattering mechanism at LT, around the CNP [19]. Since the momentum scattering mechanism is different near CNP at LT, it is not surprising that the spin scattering mechanism is also different. We note that two mysteries remain to be resolved: why is a transition to the different spin scattering mechanism observed in BLG (1) near CNP, and (2) only at LT. One possible explanation could be related to the thermally activated nature of carriers in this density regime.

In conclusion, we have demonstrated spin injection and detection in BLG across MgO barriers and observed spin-relaxation times up to 2 ns at room temperature. Our systematic study shows that at RT spin scattering in BLG follows an inverse dependence of τ_s on both the mobility μ and the room temperature σ_{\min} , indicating a DP spin scattering mechanism. We discuss the role of intrinsic and extrinsic factors that could lead to the dominance of DP spin scattering in BLG. While the inverse scaling of mobility with τ_s persists down to 5 K, the density dependence of τ_s indicates deviations from DP mechanism at these low temperatures near the charge neutrality point.

The Aachen team acknowledges support by DFG through FOR 912. B.B and M.P. acknowledge support from JARA-FIT. The Singapore team acknowledges support by the Singapore National Research Foundation under NRF RF No. NRF-RF2008-07, NRF-R-143-000-360-281, U.S. Office of Naval Research (ONR and ONR Global), and by NUS NanoCore.

Note added.—Recently, related works on BLG and on multilayer graphene became available [30,31].

*tsungyang@physik.rwth-aachen.de

†jayakumar.b@gmail.com

‡bernd.beschoten@physik.rwth-aachen.de

§barbaros@nus.edu.sg

- [1] N. Tombros *et al.*, *Nature (London)* **448**, 571 (2007).
- [2] N. Tombros *et al.*, *Phys. Rev. Lett.* **101**, 046601 (2008).
- [3] C. Jozsa *et al.*, *Phys. Rev. Lett.* **100**, 236603 (2008).
- [4] C. Jozsa *et al.*, *Phys. Rev. B* **80**, 241403 (2009).
- [5] S. Cho, Y.-F. Chen, and M. S. Fuhrer, *Appl. Phys. Lett.* **91**, 123105 (2007).
- [6] W. Han *et al.*, *Appl. Phys. Lett.* **94**, 222109 (2009).
- [7] W. Han *et al.*, *Phys. Rev. Lett.* **102**, 137205 (2009).
- [8] K. Pi *et al.*, *Phys. Rev. Lett.* **104**, 187201 (2010).
- [9] W. Han *et al.*, *Phys. Rev. Lett.* **105**, 167202 (2010).
- [10] M. Shiraishi *et al.*, *Adv. Funct. Mater.* **19**, 3711 (2009).
- [11] A. H. Castro Neto and F. Guinea, *Phys. Rev. Lett.* **103**, 026804 (2009).
- [12] D. Huertas-Hernando, F. Guinea, and A. Brataas, *Phys. Rev. Lett.* **103**, 146801 (2009).
- [13] K. S. Novoselov *et al.*, *Science* **306**, 666 (2004).
- [14] A. H. Castro Neto *et al.*, *Rev. Mod. Phys.* **81**, 109 (2009).
- [15] C. Ertler *et al.*, *Phys. Rev. B* **80**, 041405 (2009).
- [16] S. Das Sarma, E. H. Hwang, and E. Rossi, *Phys. Rev. B* **81**, 161407 (2010).
- [17] S. Adam and M. D. Stiles, *Phys. Rev. B* **82**, 075423 (2010).
- [18] F. Guinea, *New J. Phys.* **12**, 083063 (2010).
- [19] See Supplemental Material at <http://link.aps.org/supplemental/10.1103/PhysRevLett.107.047206> for detailed descriptions.
- [20] R. J. Elliott, *Phys. Rev.* **96**, 266 (1954).
- [21] M. I. D'yakonov and V. I. Perel, *Sov. Phys. Solid State* **13**, 3023 (1972).
- [22] M. Monteverde *et al.*, *Phys. Rev. Lett.* **104**, 126801 (2010).
- [23] In addition the Co electrodes induce some distortion on the hole side of the R_{sq} vs V_G .
- [24] F. J. Jedema *et al.*, *Nature (London)* **416**, 713 (2002).
- [25] We note that there are small-amplitude oscillations on top of the Hanle signal, which we only observe for the sample with the longest τ_s . A similar effect has been reported in Ref. [2].
- [26] J. C. Meyer *et al.*, *Solid State Commun.* **143**, 101 (2007).
- [27] S. Xiao *et al.*, *Phys. Rev. B* **82**, 041406 (2010).
- [28] S. V. Morozov *et al.*, *Phys. Rev. Lett.* **100**, 016602 (2008).
- [29] J. Nilsson *et al.*, *Phys. Rev. Lett.* **97**, 266801 (2006).
- [30] W. Han and R. K. Kawakami, following Letter, *Phys. Rev. Lett.* **107**, 047207 (2011).
- [31] T. Maassen *et al.*, *Phys. Rev. B* **83**, 115410 (2011).